

Catalytic oxidation of organic sulfides by new iron-chloro Schiff base complexes: The effect of methoxy substitution and ligand isomerism on the electronic, electrochemical and catalytic performance of the complexes



Fatemeh Aghvami^a, Abolfazl Ghaffari^a, Monika Kucerakova^b, Michal Dusek^b, Rahman Karimi-Nami^c, Mojtaba Amini^{c,d}, Mahdi Behzad^{a,*}

^a Faculty of Chemistry, Semnan University, Semnan 35351-1911, Iran

^b Institute of Physics ASCR, v.v.i, Na Slovance 2, 182 21 Praha 8, Czech Republic

^c Department of Chemistry, Faculty of Science, University of Maragheh, Maragheh, Iran

^d Department of Inorganic Chemistry, Faculty of Chemistry, University of Tabriz, Tabriz, Iran

ARTICLE INFO

Article history:

Received 3 January 2021

Accepted 25 February 2021

Available online 5 March 2021

Keywords:

Catalysis
Iron-chloro
Schiff base
Sulfoxidation

ABSTRACT

Four new Fe(III)-Chloro Schiff base complexes were synthesized and characterized. The N₂O₂ type tetradentate Schiff base ligands were synthesized from the condensation of *meso*-1,2-diphenyl-1,2-ethylenediamine with salicylaldehyde (**H₂L¹**), 3-methoxysalicylaldehyde (**H₂L²**), 4-methoxysalicylaldehyde (**H₂L³**) and 5-methoxysalicylaldehyde (**H₂L⁴**). The corresponding iron-chloro complexes with the general formula [Fe(Lⁿ)Cl] (n = 1–4 for complexes **(1–4)**) were characterized by FTIR and UV–Vis spectroscopy and elemental analysis. Crystal structure of **(1)** was obtained by single-crystal X-ray crystallography. Cyclic voltammetry was used to study the electrochemistry of the complexes. The complexes were used as catalysts for the selective oxidation of organic sulfide compounds to sulfoxides. High catalytic performance and selectivity were obtained. The spectroscopic, electrochemical and catalytic data are discussed based on the electronic, steric and electrochemical properties of the complexes.

© 2021 Elsevier Ltd. All rights reserved.

1. Introduction

Sulfoxides are great chemicals. They are used as intermediates in the synthesis of a variety of important materials and are also found as the main structure of some drugs [1–3]. Omeprazole, esomeprazole and armodafinil are just three examples. Selectively converting sulfides to sulfoxides is an interesting reaction. Over the past decades, several transition metal complexes have been employed for the catalytic transformation of organic compounds to more valuable materials, including the selective transformation of sulfides to sulfoxides [7–10]. Iron containing enzymes catalyze several reactions such as oxygen activation and insertion into organic compounds [4–6]. Selectivity and rapid catalysis are two most important characteristics of enzymatic reactions. Hence, the designation and study of new materials with the same characteristics is an interesting and challenging field of study. In this regard, nitrogen containing ligands have gained great interest [11].

Schiff base ligands are nitrogen containing ligands that could be easily synthesized and their stereo-electronic properties could be easily tuned by using different amines or aldehydes. Various transition metal Schiff base complexes have been employed for the preparative oxidation of sulfides, including Co, Mn, Cu, Ni and Fe [12–16]. Among them, less attention has been paid to the Fe(III) Schiff base complexes. Hence, herein we report the synthesis, characterization and electrochemistry of four new Fe(III)-chloro complexes of tetradentate N₂O₂ type Schiff base ligands. Crystal structure of one of the complexes, i.e. **(1)**, was also obtained. The new complexes were used for catalytic oxidation of sulfides. Methylphenylsulfide (MPS) and **(1)** were used as model substrate and catalyst, and urea hydroperoxide (UHP) was used as the oxidant. Various reaction conditions were optimized. It was proven that the complexes showed good catalytic activity and sulfoxide selectivity. Electronic and electrochemical behaviors of the complexes were rationalized based on the presence and location of the substituted methoxy group.

* Corresponding author.

E-mail address: mbehzad@semnan.ac.ir (M. Behzad).

2. Experimental

2.1. Materials and methods

All of the used chemicals and solvents were purchased from commercial sources and were used as received. *Meso*-1,2-diphenyl-1,2-ethylenediamine [17] and the Schiff base ligands H_2L^1 - H_2L^4 were synthesized as described elsewhere [18]. FT-IR spectra were obtained as KBr plates using a Shimadzu FT-IR instrument. UV-Vis spectra were obtained on a Shimadzu UV-1650 PC spectrophotometer. Elemental analyses were performed on a Perkin-Elmer 2400II CHNS-O analyzer. The X-ray diffraction measurements were carried out on a SuperNova diffractometer of Rigaku Oxford Diffraction. A Metrohm 757 VA computerized instrument was employed to obtain cyclic voltammograms in freshly prepared acetonitrile solutions at room temperature (25 °C) using 0.1 M tetra-*n*-butylammonium hexafluorophosphate (TBAHFP) as supporting electrolyte. The solutions were purged with N_2 for at least 10 min to remove any dissolved O_2 . A platinum working electrode, a platinum auxiliary electrode and an Ag/AgCl reference electrode were used to obtain cyclic voltammograms in the range of -1 to +1 V. The ferrocenium/ferrocene redox couple was used as the internal reference for the potential measurements.

2.2. General synthesis of the complexes

The complexes were prepared following a general procedure for similar complexes [19,20]. Typically, 1.00 mmol of each ligand (see Scheme 1) was dissolved in 40 mL of warm ethanol in a round bottom flask. 1.00 mmol of $FeCl_3 \cdot 6H_2O$ (0.27 g), dissolved in 20 mL of ethanol, was then added to the ligand solution and the reaction

mixture was refluxed and stirred for six hours. The progress of the reaction was monitored by TLC. The resulting brown precipitates were filtered off, washed with ethanol and air-dried. The precipitates were then recrystallized from $CHCl_3$ to obtain pure target complexes.

2.2.1. $[Fe(L^1)Cl] \cdot CHCl_3$ (1)

Yield: 0.52 g, 82%. Anal. Calcd. for $C_{28}H_{22}ClFeN_2O_2 \cdot CHCl_3$: C: 55.31; H: 3.65; N: 4.45. Found: C: 55.70; H: 3.94; N: 4.90. Selected IR (cm^{-1}): 1602, 1539, 1434 and 1294. UV-Vis. 10^{-5} M solution in CH_3CN [λ_{max} nm, (ϵ $M^{-1}cm^{-1}$)]: 236 (39,400), 268 (8900), 326 (11,500), 494 (3800).

2.2.2. Synthesis of $[Fe(L^2)Cl] \cdot H_2O$ (2)

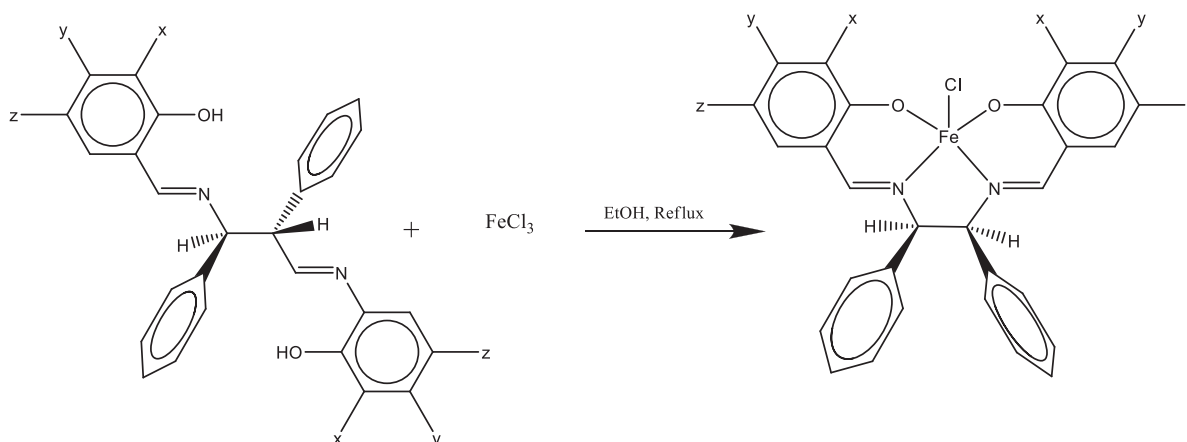
Yield: 0.54 g, 87%. Anal. Calcd. for $C_{30}H_{28}ClFeN_2O_5$: C: 61.29; H: 4.80; N: 4.77. Found: C: 61.70; H: 4.59; N: 4.63. Selected IR (cm^{-1}): 1602, 1435, and 1255. UV-Vis. 10^{-5} M solution in CH_3CN [λ_{max} nm, (ϵ $M^{-1}cm^{-1}$)]: 232 (49,200), 276 (26,000), 368 (16,000), 454 (3970), 530 (2300).

2.2.3. Synthesis of $[Fe(L^3)Cl]$ (3)

Yield: 0.53 g, 85%. Selected IR (cm^{-1}): 1587, 1525 and 1226. UV-Vis. 10^{-5} M solution in CH_3CN [λ_{max} nm, (ϵ $M^{-1}cm^{-1}$)]: 250 (47,800), 278 (43,800), 386 (7500), 400 (6300), 492 (5400). Anal. Calcd. For $C_{30}H_{26}ClFeN_2O_4$ (%): C, 63.01; H, 4.60; N, 4.90. Found: C, 63.22; H, 4.40; N, 5.01.

2.2.4. Synthesis of $[Fe(L^4)Cl]$ (4)

Yield: 0.50 g, 81%. Selected IR (cm^{-1}): 1593, 1535, 1458 and 1288. UV-Vis. 10^{-5} M solution in CH_3CN [λ_{max} nm, (ϵ $M^{-1}cm^{-1}$)]: 250 (36,500), 274 (25,300), 330 (9300), 396 (6100), 524 (4900).



Ligand	Complex	x	y	z
H_2L^1	(1)	H	H	H
H_2L^2	(2)	OCH ₃	H	H
H_2L^3	(3)	H	OCH ₃	
H_2L^4	(4)	H	H	OCH ₃

Scheme 1. Reaction pathway for the synthesis of the complexes.

Anal. Calcd. For $C_{30}H_{26}ClFeN_2O_4$ (%): C, 63.01; H, 4.60; N, 4.90. Found: C, 62.88; H, 4.48; N, 5.15.

2.3. X-ray crystallography

Diffraction data from selected single crystal of (**1**) with dimensions $0.102 \times 0.073 \times 0.033$ mm were collected at 95 K on SuperNova (Rigaku Oxford Diffraction) microsource diffractometer equipped with a CCD detector Atlas S2, using $CuK\alpha$ radiation. Structure was solved with SHELXT [21] and refined with Jana2006 [22]. The process of structure solution and refinement was standard; hydrogen atoms on carbon were refined as riding atoms.

2.4. General procedure for the sulfide oxidation

To a solution of sulfide (0.2 mmol), chlorobenzene (0.2 mmol) as internal standard, and catalyst (0.005 mmol) in a 1:1 mixture of CH_3OH/CH_2Cl_2 (1 mL) as solvent was added 0.4 mmol UHP as an oxidant. After stirring the mixture at room temperature, the reaction progress was monitored by GC, and oxidation products were assigned by matching with authentic samples (Scheme 2).

3. Results and discussions

3.1. Description of the crystal structure

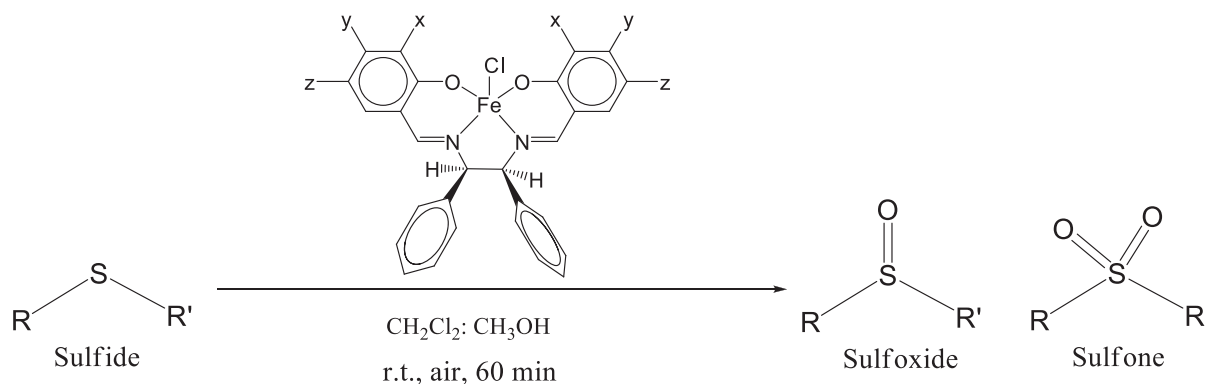
Fig. 1 shows the molecular structure of the complex (**1**), i.e. $[Fe(L^1)Cl] \cdot CHCl_3$ with common atom numbering scheme. Tables 1 and 2 summarize the crystallographic data and selected bond lengths and bond angles, respectively. This complex is neutral in which a doubly deprotonated Schiff base ligand (L^{2-}) and a chloro (Cl^-) ligand are coordinated to a central Fe(III) metal ion. The geometry around the central metal ion is a square-based pyramid (SBP) with N_2O_2 coordinating atoms of the Schiff base ligand at basal positions, and the chloro ligand at the axial position. The N_2O_2 coordinating atoms comprise two iminic nitrogen atoms and two deprotonated phenolic oxygen atoms. The central metal ion is located 0.488 Å above the basal plane of the square pyramid. Consequently, $Cl-Fe-N$ and $Cl-Fe-O$ angles are larger than 90° . The average $Fe-N$, $Fe-O$ and $Fe-Cl$ bond lengths are in the common range of the previously reported similar complexes [23–27]. The τ_5 geometry index calculated from $(\beta-\alpha)/60$ is equal to 0.25. In this equation, β and α are the two greatest angles around the central metal ion. The τ value can range from 0 to 1, where zero stands for an ideal SBP while 1 indicates ideal trigonal bipyramidal geometry [28]. Thus the coordination polyhedron could be considered as a distorted SBP.

The packing of the complex is governed by hydrogen bond $C2-H1C3 \cdots Cl1$ [distance $D \cdots A$ 3.439(2) Å, angle $D-H \cdots A = 126^\circ$]; $\pi \cdots \pi$ interaction between aromatic rings Cg5 [Cg5 = C4, C8, C22, C19, C23, C24, distance $Cg5 \cdots Cg5 = 3.6614(12)$ Å]; $C25-H1C25 \cdots Cg5$ interaction [distance $C25 \cdots Cg5 = 3.474(2)$ Å]; $C8-H1C8 \cdots Cg7$ interaction [Cg7 = C11, C13, C29, C27, C20, C15, distance $C8 \cdots Cg7 = 3.738(3)$ Å]; and $C18-Cl3 \cdots Cg4$ interaction [Cg4 = C2, C28, C10, C6, C12, distance $Cl \cdots Cg4 = 3.5933(12)$ Å]. These interactions shown in Fig. 2 connect molecules into a slab extended along a (Supplemental Fig. S.1). No remarkable interaction was found between the slabs.

3.2. Spectroscopic characterization

The complexes were synthesized following a general route for the synthesis of Fe(III)-chloro Schiff base complexes and were characterized by different spectroscopic and analytical methods. The FTIR spectra of the synthesized complexes (see Supplemental Fig. S.2–5) showed a strong signal at around 1600 cm^{-1} which is assignable to the stretching vibration of the imine group $\nu(C=N)$. This is the most characteristic signal in the FTIR spectra of such complexes and clearly confirms the synthesis of the Schiff bases. Comparison of this signal with the $\nu(C=N)$ of the previously reported corresponding ligands [18] showed that this signal is shifted by about 30 cm^{-1} to lower wavenumbers in the complexes, which confirms the coordination through the iminic nitrogen atoms. This shift to lower wavenumbers is due to the π -back donation of electron density from the central metal ion to the π^* orbitals of the imines which weakens the mentioned bond. Interestingly, the $[Fe(L^3)Cl]$ complex (**3**), in which the OMe is located trans to the $C=N$, has the lowest $\nu(C=N)$. We have previously shown that the presence of OMe trans to $C=N$ results in the transfer of electron density to $\pi^*(C=N)$, and causes a decrease in the wavenumber [18]. The signals observed at around 1535 and 1435 cm^{-1} could be attributed to $\nu(C=C)$ and the signal at around 1250 cm^{-1} is also assignable to $\nu(C-O)$.

The UV-Vis spectra of the four ligands were quiet similar and have been reported earlier [18]. Two intense signals at around 300 and 250 nm in those ligands had been assigned to the $\pi \rightarrow \pi^*$ transitions of the azomethine and the aromatic ring, respectively. In the UV-Vis spectra of the complexes (See Supplemental Fig. S.6), the former signal is blue-shifted by about 20–30 nm, which confirms the coordination through the azomethine nitrogen atoms. The electronic spectra of the complexes exhibited signals above 300 nm with lower intensity than the $\pi \rightarrow \pi^*$ transitions in the same complex, which could be assigned to the LMCT from the orbital mainly located on the central metal ion to the orbital mainly located on the azomethine π^* [27–30]. In the complex with



Scheme 2. General oxidation pathway.

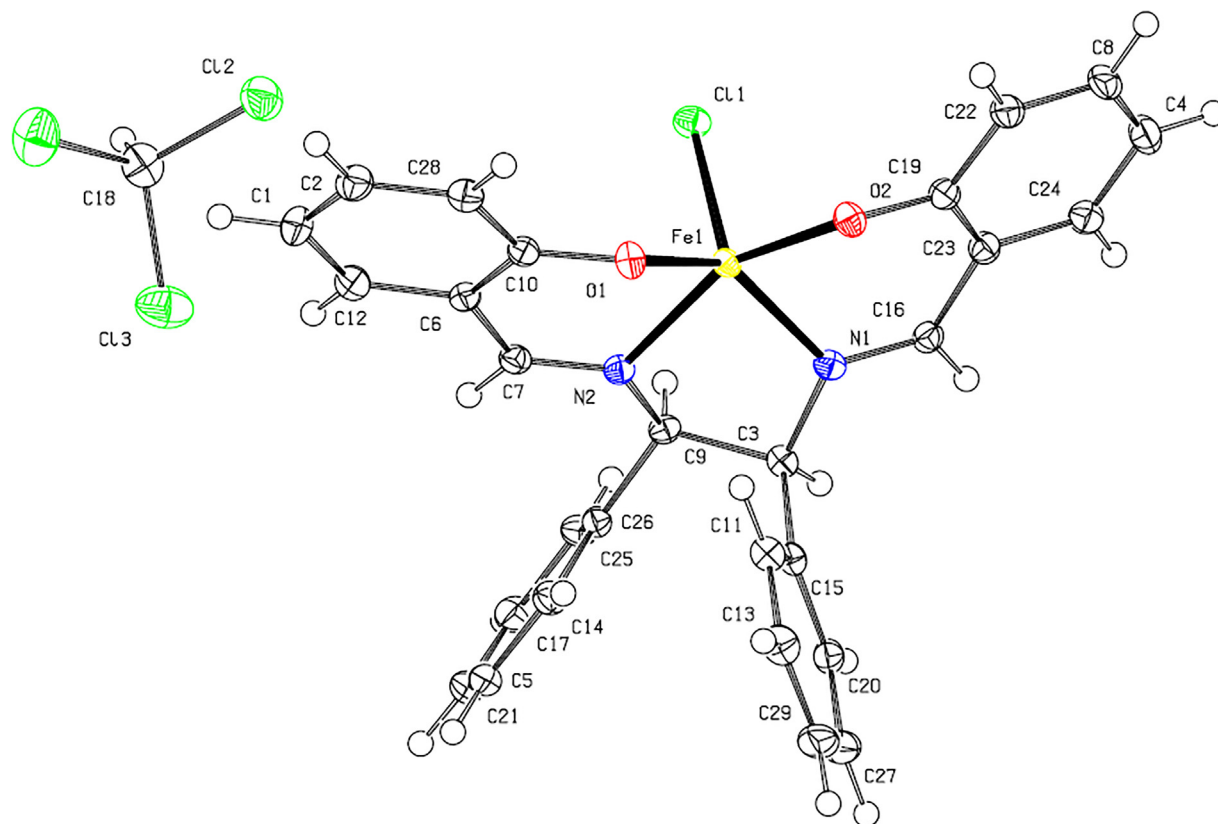


Fig. 1. Molecular structure of complex $[\text{Fe}(\text{L}^1\text{Cl})\text{Cl}]\cdot\text{CHCl}_3$ (**1**). Thermal ellipsoids are drawn at 50% probability level, and hydrogen atoms are drawn as spheres of arbitrary radii.

Table 1
Experimental crystallographic details.

Crystal data	$[\text{Fe}(\text{L}^1\text{Cl})\text{Cl}]\cdot\text{CHCl}_3$
Chemical formula	$\text{C}_{29}\text{H}_{25}\text{Cl}_4\text{Fe}_1\text{N}_2\text{O}_2$
M_r	629.2
Crystal system, space group	Triclinic, $P\bar{1}$
Temperature (K)	95.00(10)
a, b, c (Å)	10.5789(3), 10.7786(2), 14.4673(4)
A, β, γ (°)	76.458(2), 72.098(3), 62.746(3)
V (Å ³)	1386.98(7)
Z	2
Radiation type	Cu $K\alpha$
μ (mm ⁻¹)	8.15
Crystal size (mm)	0.10 × 0.07 × 0.03
$T_{\text{min}}, T_{\text{max}}$	0.697, 1
No. of measured, independent and observed [$I > 3\sigma(I)$] reflections	8289, 5389, 4722
R_{int}	0.022
$R[F^2 > 3\sigma(F^2)], wR(F^2), S$	0.030, 0.040, 1.63
No. of reflections	5389
No. of parameters	343
$\Delta\rho_{\text{max}}, \Delta\rho_{\text{min}}$ (e Å ⁻³)	0.36, -0.30

no methoxy substituents, i.e. (**1**), the higher energy signal in this region observed at 326 nm but in the complexes with methoxy substituents, this band is red shifted. In (**3**) in which the OMe is located trans to the C=N group, this signal is observed at 386 nm which shows the highest red shift. This is consistent with the above mentioned IR result for the same complex. Hence, the location of OMe has shown a drastic effect on the LMCT bands, which further confirms our previous study [18]. Other LMCT transitions, which could be mixed with spin forbidden $d \rightarrow d$ transitions, in these complexes are also observed above 400 nm. These signals are

Table 2
Selected bond lengths and bond angles around the central metal ion.

Bond lengths (Å)		Bond angles (°)	
Fe1–Cl1	2.2335 (5)	Cl1–Fe1–O1	109.22 (4)
Fe1–O1	1.8941 (14)	Cl1–Fe1–O2	104.47 (4)
Fe1–O2	1.895 (2)	Cl1–Fe1–N1	106.82 (4)
Fe1–N1	2.0750 (16)	Cl1–Fe1–N2	95.88 (5)
Fe1–N2	2.091 (2)	O1–Fe1–O2	95.10 (8)
		O1–Fe1–N1	142.06 (6)
		O1–Fe1–N2	87.49 (8)
		O1–Fe1–N2	87.02 (8)
		O2–Fe1–N2	157.29 (6)
		N1–Fe1–N2	77.39 (8)

observed as two split signals in the OMe substituted complexes but as a very broad band centered at around 500 nm in (**1**). Again the lowest energy transition has shown a blue shift due to the location of C=N [27]. The obtained results are similar to the previously reported complexes with similar structures [27,30].

3.3. Cyclic voltammetry

The electrochemical behavior of the $[\text{Fe}(\text{L}^n)\text{Cl}]$ complexes ($n = 1-4$) was studied by means of cyclic voltammetry, and the results are shown as Supplemental Fig. S.7 and are summarized in Table 3. The complexes showed a reversible or a quasi-reversible reduction potential due to Fe(III)/Fe(II) redox couple [29–31]. As could be seen from Table 3, the results of the CV studies are also consistent with the results of spectroscopic studies. Again the $[\text{Fe}(\text{L}^3)\text{Cl}]$ complex (**3**) showed the most negative standard reduction potential which is due to the para location of the OMe to C=N, which has resulted in the transfer of electron density to Fe(III). This results in the stabilization of Fe(III) and hence, its lower tendency

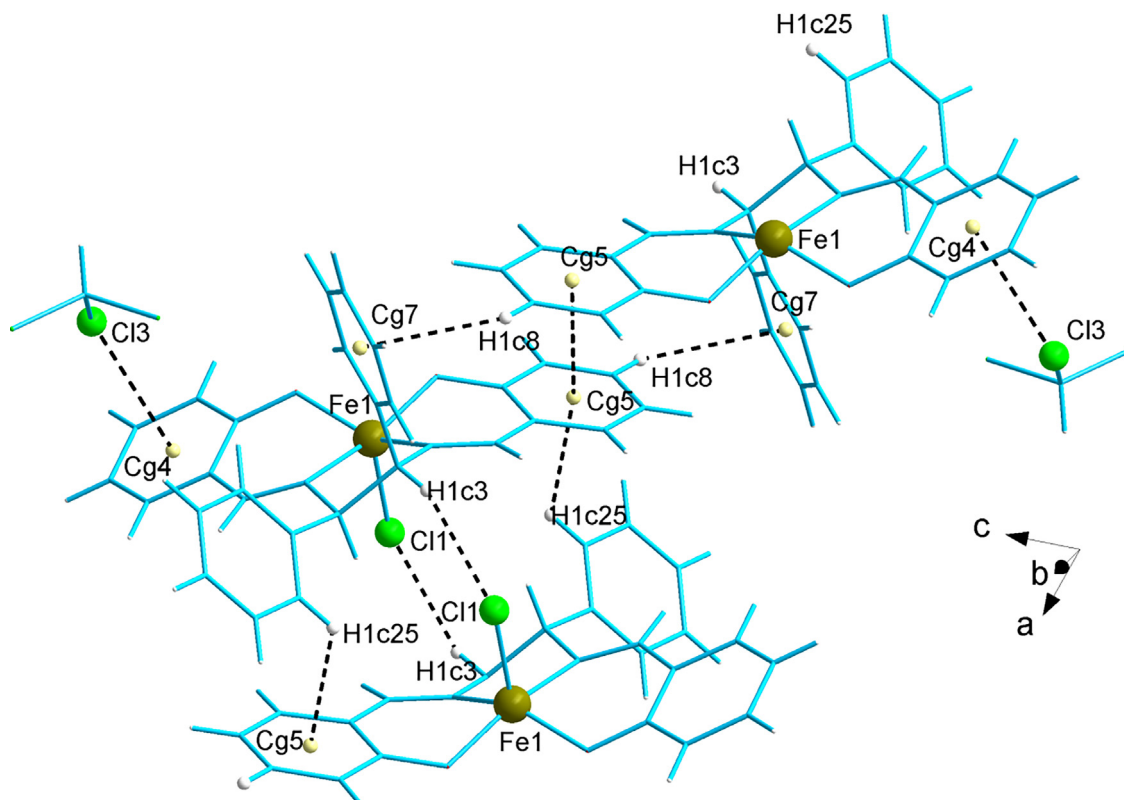


Fig. 2. Weak interactions influencing packing of the complex (**1**). Centroids Cg4, Cg5 and Cg7 as well as and geometric characteristics of the interactions are given in the text. Atoms and centroids participating in the interactions and atoms of iron are indicated as balls and labeled.

Table 3

The cyclic voltammetry data for the new complexes in CH_3CN (10^{-3} M) containing 0.1 M tetra-*n*-butylammoniumhexafluorophosphate as supporting electrolyte.

Complex	E^0 (V)	E^c (V)	E^a (V)	ΔE (V)
(1)	-0.656	-0.677	-0.635	0.042
(2)	-0.240	-0.285	-0.196	0.089
(3)	-0.820	-0.909	-0.730	0.179
(4)	-0.280	-0.315	-0.244	0.071

to reduction. Complexes (**2**) and (**4**) with OMe substitution in the meta position of the C=N have almost similar E^0 value and more positive values.

3.4. Catalysis

MPS was used as the model substrate for catalytic oxidation of sulfides using complex (**1**) as a model catalyst and UHP as oxidant. Various reaction conditions, including catalyst amount, oxidant amount, solvent type and reaction time were optimized. The results are summarized in Table 4. As could be seen from entry **1** of this table, in the absence of the catalyst, trace amount of the product was observed, while by increasing the catalyst up to 5 μmol , the yield of the product was increased. Besides, excellent selectivity to sulfoxide was also observed. The solvent type also had a dramatic effect on catalytic activity. As could be seen from entries **11–15**, in the presence of the used single solvents, the conversion was not high enough, but in the 1:1 CH_2Cl_2 : CH_3OH solvent, the conversion was increased. Nonpolar solvents such as dichloromethane and chloroform are not the preferred solvents for sulfide oxidation, but the better solubility of the complex in these solvents had prompted us to test mixed polar-nonpolar solvent CH_2Cl_2 : CH_3OH for this reaction, and the best results were obtained in this mixture.

The increase in UHP amount up to 0.4 mmol also affected and increased the catalytic activity. Reaction time was also optimized, and the best results were obtained in 60 min reaction time.

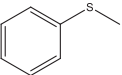
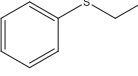
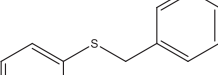
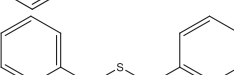
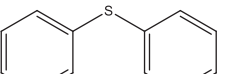
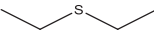
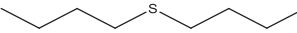
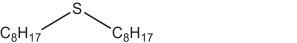
The study of the effect of different substituents on the catalytic transformation of organic compounds is an interesting field of study [32–34]. Hence, in order to investigate the effect of the presence of the methoxy substitutions, as well as their position, i.e. ligand isomerism, on the catalytic activity of the new Schiff base complexes, the catalytic activity of other complexes was also studied using the optimized conditions for (**1**), and the results are collected in Table 5. As could be seen from Table 5, complexes (**1**) and (**4**) showed almost higher activity than complexes (**2**) and (**3**). This means that the steric effect of the OMe substituents mainly governs the catalytic behavior of the complexes. Complex (**1**) with no OMe substituents and (**4**) in which OMe's are located far from the central metal ion showed higher catalytic activity which supports the steric effect of the OMe substituents. Complex (**2**) in which OMe substituents are at the closest location of the central metal ion showed the least activity. Other stereo-electronic factors may also be important; for example, it could be seen from Table 3 that the complexes with higher reversibility in cyclic voltammetry have shown greater catalytic activity. We are currently synthesizing new complexes to further investigate this idea.

Table 4
The effect of various conditions in the oxidation of methylphenylsulfide by (1)/UHP.

Entry	Amount of catalyst (mmol)	Amount of UHP (mmol)	Solvent (1 mL)	Time (min)	Conversion (%)	Selectivity to Sulfoxide (%) ^a
1	0	0.4	CH ₂ Cl ₂ :CH ₃ OH	60	Trace	–
2	0.001	0.4	CH ₂ Cl ₂ :CH ₃ OH	60	13	100
3	0.003	0.4	CH ₂ Cl ₂ :CH ₃ OH	60	48	100
4	0.005	0.4	CH ₂ Cl ₂ :CH ₃ OH	60	79	97
5	0.007	0.4	CH ₂ Cl ₂ :CH ₃ OH	60	75	96
6	0.005	0.1	CH ₂ Cl ₂ :CH ₃ OH	60	21	100
7	0.005	0.2	CH ₂ Cl ₂ :CH ₃ OH	60	42	100
9	0.005	0.3	CH ₂ Cl ₂ :CH ₃ OH	60	65	98
10	0.005	0.5	CH ₂ Cl ₂ :CH ₃ OH	60	86	88
11	0.005	0.4	CH ₂ Cl ₂	60	17	100
12	0.005	0.4	CHCl ₃	60	15	100
13	0.005	0.4	CH ₃ CN	60	51	96
14	0.005	0.4	CH ₃ OH	60	60	95
15	0.005	0.4	CH ₃ COCH ₃	60	58	99
16	0.005	0.4	CH ₂ Cl ₂ :CH ₃ OH	30	53	99
17	0.005	0.4	CH ₂ Cl ₂ :CH ₃ OH	45	67	97

Substrate = methylphenylsulfide = 0.2 mmol.

^aSelectivity to sulfoxide = (sulfoxide%/(sulfoxide% + sulfone%)) × 100.**Table 5**
Oxidation of sulfides catalyzed by the complexes (1–4)/UHP.^a

Entry	Substrate	Conversion (%) ^b (Selectivity (%) ^c)			
		1	2	3	4
1		79(97)	65(98)	68(97)	77(98)
2		75(98)	67(98)	69(98)	77(97)
3		71(98)	60(97)	65(99)	68(99)
4		81(96)	64(98)	72(97)	75(97)
5		59(99)	66(98)	65(98)	70(98)
6		45(100)	41(100)	36(100)	38(100)
7		39(100)	35(100)	39(100)	36(100)
8		37(100)	27(100)	40(100)	33(100)

^a The molar ratios for complexes (1–4):substrate:oxidant are 1:20:40. The reactions were performed in (1:1) mixture of CH₂Cl₂/CH₃OH (1 mL) under air at room temperature within 60 min.^b The GC yield (%) are measured relative to the starting sulfide.^c Selectivity to sulfoxide = (sulfoxide%/(sulfoxide% + sulfone%)) × 100.

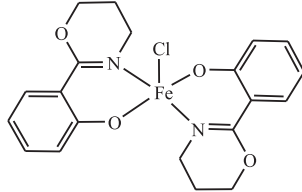
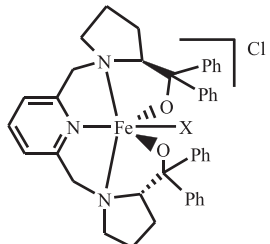
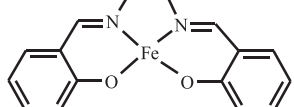
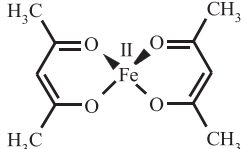
To demonstrate the superior properties of these prepared complexes, the activity of catalyst **1** was compared with some of the previously reported iron-containing complexes. The relevant comparison is given in Table 6. According to Table 6, Catalyst (**1**) is superior to previous works in terms of having the highest selectivity in reactions (entries 1–5), low reaction time (entries 3–5) and low solvent consumption in the oxidation reactions (entries 3–5).

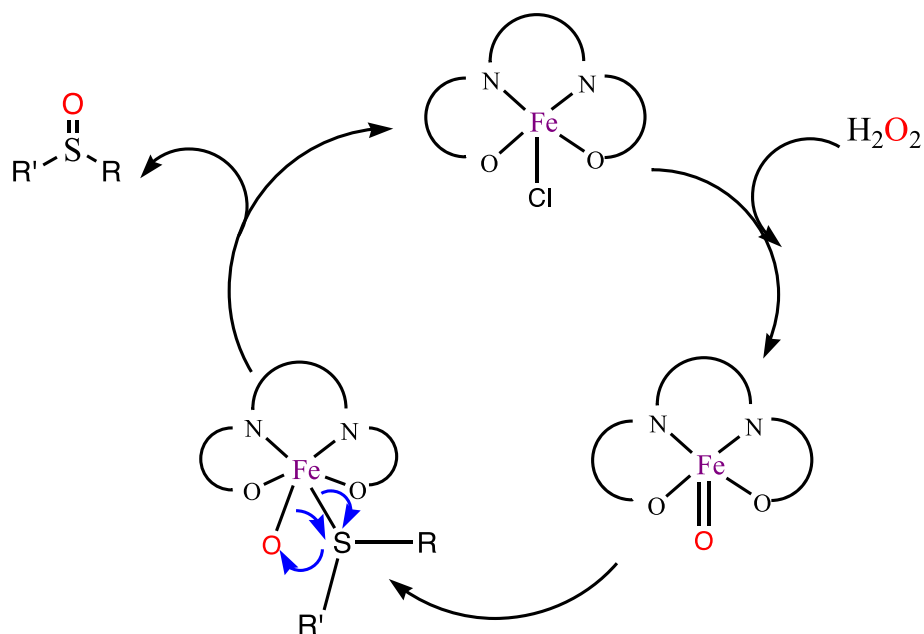
According to the previously reported works, a mechanism was proposed for the sulfide oxidation catalyzed by catalyst (**1**) [39]. By the addition of UHP, a Fe=O bond is formed on the iron complex that reaction of organic sulfide to the Fe=O can lead to the production of sulfoxide and the primary catalyst (Scheme 3).

4. Conclusion

Four new iron-chloro complexes with tetradentate N₂O₂ Schiff base ligands were synthesized and used as catalyst for selective oxidation of organic sulfides. The electronic spectroscopic data, the electrochemical data and the catalytic performance of the complexes were rationalized based on the presence and the position of methoxy substituents on the Schiff base ligand. The complexes showed good catalytic potential in the selective oxidation of organic sulfides to sulfoxides and it was proven that ligand isomerism has a considerable effect on electronic, electrochemical and catalytic properties in such complexes.

Table 6
Recently reported catalytic systems for the sulfides oxidation in the presence of iron-containing complexes.

Entry	Catalyst	Condition	Conversion (%)	Selectivity (%)	Ref.
1		The molar ratios for catalyst: substrate: UHP are 1:20:40; (CH_2Cl_2 : CH_3OH (1 mL); 60 min; at room temperature)	79	97	Present work
2		The molar ratios for catalyst: substrate: UHP are 1:20:40; (CH_2Cl_2 : CH_3OH (1 mL); 15 min; at room temperature).	85	86	[35]
3		The molar ratios for catalyst: substrate are 1:60:50; (anisic acid (10 equiv.) as an additive, CH_3CN (4 mL); 60 min; at room temperature)	85	93	[36]
4		The molar ratios for catalyst: substrate: H_2O_2 are 1:25:25; (CH_3CN (5 mL) at room temperature).	94	-	[37]
5		The molar ratios for catalyst: substrate are 1:50; (O_2 (2 MPa) PEG-1000 (0.3 g), 120 min; at 100 °C)	100	94	[38]



Scheme 3. The proposed mechanisms for oxidation of the sulfides catalyzed by (1).

Declaration of Competing Interest

The authors declare that they have no known competing financial interests or personal relationships that could have appeared to influence the work reported in this paper.

Appendix A. Supplementary data

CCDC number 1900764 contains the supplementary crystallographic data for **[Fe(L¹)Cl]·CHCl₃**. These data can be obtained free of charge from The Cambridge Crystallographic Data Centre via www.ccdc.cam.ac.uk/data_request/cif. Supplementary data to this article can be found online at <https://doi.org/10.1016/j.poly.2021.115135>.

References

- [1] M. Feng, B. Tang, S.H. Liang, X. Jiang, *Curr. Top. Med. Chem.* 16 (2016) 1200–1216.
- [2] M. Frings, C. Bolm, A. Blum, C. Gnam, *Eur. J. Med. Chem.* 126 (2017) 225–245.
- [3] H. Naslhajian, M. Amini, M.A. Dastyar, A. Bayrami, M. Bagherzadeh, S.M.F. Farnia, J. Janczak, *Polyhedron* 186 (2020) 114622.
- [4] J. Kaplan, D.M. Ward, *Curr. Biol.* 23 (2013) R642–R646.
- [5] L.D. Slep, F. Nesse, *Angew. Chem. Int. Ed. Engl.* 42 (2003) 2942–2945.
- [6] S.P. de Visser, D. Kumar, Iron-containing enzymes: versatile catalysts of hydroxylation reactions in nature, *RSC* (2011), <https://doi.org/10.1039/9781849732987>.
- [7] K. Kaczorowska, Z. Kolarska, K. Mitka, P. Kowalski, *Tetrahedron* 61 (2005) 8315–8327.
- [8] K.C. Gupta, A.K. Sutar, C.C. Lin, *Coord. Chem. Rev.* 253 (2009) 1926–1946.
- [9] H. Liu, M. Wang, Y. Wang, R. Yin, W. Tian, L. Sun, *Appl. Organomet. Chem.* 22 (2008) 253–257.
- [10] S.C. Davidson, G. dos Passos Gomes, L.R. Kuhn, I.V. Alabugin, A.R. Kennedy, N.C. O. Tomkinson, *Tetrahedron* 78 (2021) 131784.
- [11] C. Wu, B. Liu, X. Geng, Z. Zhang, S. Liu, Q. Hu, *Polyhedron* 158 (2019) 334–341.
- [12] D. Mo, J. Shi, D. Zhao, Y. Zhang, Y. Guan, Y. Shen, H. Bian, F. Huang, S. Wu, *J. Mol. Struct.* 1223 (2021) 129229.
- [13] H. Veisi, A. Rashtiani, A. Rostami, M. Shirinbayan, S. Hemmati, *Polyhedron* 157 (2019) 358–366.
- [14] V. Mirkhani, S.h. Tangestaninejad, M. Moghadam, I. Mohammadpoor-Baltork, H. Kargar, *J. Mol. Catal. A: Chemical* 242 (2005) 251–255.
- [15] M. Khorshidifard, H. Amiri Rudbari, B. Askari, M. Sahihi, M. Riahi Farsani, F. Jalilian, G. Bruno, *Polyhedron* 95 (2015) 1–13.
- [16] E. Zamanifar, F. Farzaneh, J. Simpson, M. Maghami, *Inorg. Chim. Acta* 414 (2014) 63–70.
- [17] M.N.H. Irving, R.M. Parkins, *J. Inorg. Nucl. Chem.* 27 (1965) 270–271.
- [18] A. Ghaffari, M. Behzad, M. Pooyan, H.A. Rudbari, G. Bruno, *J. Mol. Struct.* 1063 (2014) 1–7.
- [19] Y.X. Zhou, X.F. Zheng, D. Han, H.Y. Zhang, X.Q. Shen, C.Y. Niu, P.K. Chen, H.W. Hou, Y. Zhu, *Synth. React. Inorg., Met.-Org., Nano-Met. Chem.* 36 (2006) 693–699.
- [20] Y. Kobayashi, R. Obayashi, Y. Watanabe, H. Miyazaki, I. Miyata, Y. Suzuki, Y. Yoshida, T. Shioiri, M. Matsugi, *Eur. J. Org. Chem.* 2019 (2019) 2401–2408.
- [21] G. Sheldrick, SHELXT – integrated space-group and crystal-structure determination, *Acta Crystallogr. A* 71 (2015) 3–8.
- [22] Petříček, M. Dušek, L. Palatinus, Crystallographic computing system JANA2006: general features, *Z. Kristallogr. Cryst. Mater.* 229 (2014) 345–352.
- [23] A. Ghaffari, M. Behzad, M. Pooyan, H. Amiri Rudbari, G. Bruno, *J. Mol. Struct.* 1063 (2014) 1–7.
- [24] S. Muche, K. Harms, O. Burghaus, M. Hołynska, *Polyhedron* 144 (2018) 66–74.
- [25] T. Basak, K. Ghosh, S. Chattopadhyay, *Polyhedron* 146 (2018) 81–92.
- [26] B. de P. Cardoso, A.I. Vicente, J.B.J. Ward, P.J. Sebesti, F. Vaca Chavez, S. Barroso, A. Carvalho, S.J. Keely, P.N. Martinho, M.J. Calhorda, *Inorg. Chim. Acta* 432 (2015) 258–266.
- [27] J. Cisterna, V. Artigas, M. Fuentealba, P. Hamon, C. Manzur, J.-R. Hamon, D. Carrillo, *Inorganics* 6 (2018), <https://doi.org/10.3390/inorganics6010005>.
- [28] A.W. Addison, T. Nageswara Rao, J. Reedijk, J. van Rijn, G.C. Verschoor, *J. Chem. Soc., Dalton Trans.* 1349 (1984), <https://doi.org/10.1039/dt9840001349>.
- [29] J.P. Costes, J.B. Tommasino, D. De Montauzon, *Polyhedron* 12 (1993) 641–649.
- [30] Z. Shaghaghi, R. Bikas, H. Tajdar, A. Kozakiewicz, *J. Mol. Struct.* 1217 (2020) 128431.
- [31] T. Ueda, N. Inazuma, D. Kumatsu, H. Yasuzawa, A. Onda, S.X. Guo, A.M. Bond, *Dalton Trans.* 42 (2013) 11146–11154.
- [32] R. Bikas, E. Shahmoradi, N. Noshiranzadeh, M. Emami, S. Reinoso, *Inorg. Chim. Acta* 466 (2017) 100–109.
- [33] J. Rahchamani, M. Behzad, A. Bezaatpour, V. Jahed, G. Dutkiewicz, M. Kubicki, M. Salehi, *Polyhedron* 30 (2011) 2611–2618.
- [34] R. Bikas, V. Lippolis, N. Noshiranzadeh, H. Farzaneh-Bonab, A.J. Blake, M. Siczek, H. Hosseini-Monfared, T. Lis, *Eur. J. Inorg. Chem.* 2017 (2017) 999–1006.
- [35] M. Amini, M.M. Haghdost, M. Bagherzadeh, A. Ellern, L.K. Woo, *Polyhedron* 61 (2013) 94–98.
- [36] S. Gosiewska, M. Lutz, A.L. Spek, R.J.M.K. Gebbink, *Inorg. Chim. Acta* 360 (2007) 405–417.
- [37] A.M.I. Jayaseeli, S. Rajagopal, *J. Mol. Catal. A: Chem.* 309 (2009) 103–110.
- [38] B. Li, A.-H. Liu, L.-N. He, Z.-Z. Yang, J. Gao, K.-H. Chen, *Green Chem.* 14 (2012) 130–135.
- [39] M. Amini, M.M. Najafpour, M. Zare, M. Holyńska, A.N. Moghaddam, M. Bagherzadeh, *J. Coord. Chem.* 67 (2014) 3026–3032.